Pergamon

Tetrahedron: *Asymmetry* 13 (2002) 1663–1671

TETRAHEDRON: *ASYMMETRY*

Synthesis, crystal structures and optical activity of *cis*- and *trans*-(−)-dichloro[(*S*)-methyl *p*-tolylsulfoxide]pyridyl platinum(II) complexes

Alexej N. Skvortsov,[b,*] Dimitry A. de Vekki,[a] Adam I. Stash,[c] Vitaly K. Belsky,[c] Vitaly N. Spevak[a] and Nickolaj K. Skvortsov[a]

[a]*St. Petersburg State Institute of Technology (Technical University) Moskowsky pr., 26, St. Petersburg 198013, Russia*
[b]*Institute of Cytology of the Russian Academy of Sciences, Tikhoretsky pr., 4, St.-Petersburg 194064, Russia*
[c]*L.Ya. Karpov Physico-Chemical Institute, Vorontsovo Pole st. 10, Moscow 103064, Russia*

Received 14 June 2002; accepted 23 July 2002

Abstract—The chiral mixed-ligand platinum(II) complexes *cis*- and *trans*-{Pt[(*S*)-Me-*p*-TolSO]PyCl$_2$}, which are potential catalysts for asymmetric hydrosilylation and useful tools for kinetic and mechanistic studies, were analyzed by X-ray diffraction, ^{1}H NMR and circular dichroism spectroscopy. The possibility of using the asymmetric sulfoxide as a chiral label for monitoring substitution reactions is also discussed. © 2002 Elsevier Science Ltd. All rights reserved.

1. Introduction

Mixed-ligand sulfoxide complexes of platinum(II) attract considerable interest because of their catalytic properties in hydrosilylation processes[1–4] and the strong cytotoxic activity of some species towards cancer cell lines which are resistant to the widely used anti-cancer drug cisplatin.[5–7] The common mechanism underlying both the catalytic activity and the cytotoxic properties of platinum complexes is ligand exchange. Thus, the efficiency of platinum catalysts as well as the toxicity and selectivity of platinum anti-cancer drugs is determined by their ability to undergo specific ligand exchange reactions and their stability towards undesired side reactions. The low working concentrations of platinum catalysts and drugs make the study of these reactions difficult and the extrapolation of results obtained at higher concentrations is not always valid. Complexes containing chiral sulfoxide ligands have the advantage of being detectable by their optical activity. The chiral sulfoxide (*R*)-(+)-methyl-*p*-tolylsulfoxide (Me-*p*-TolSO, (*R*)-1-methylsulfinyl-4-methylbenzene) proved to be a very useful chiral label for studying ligand exchange at relevant concentrations by circular dichroism (CD) spectroscopy and optical rotation measurements.[8–11] A number of complexes with Me-*p*-TolSO were characterized previously[12–16] and the structure of the ligand[17] and some complexes was determined by X-ray analysis. Known structures include sulfoxide–olefin complexes,[12,13] bis-sulfoxide complexes such as *cis*-{Pt[(*S*)-Me-*p*-TolSO]$_2$Cl$_2$}[14] and *cis*-{Pt[(*S*)-Me-*p*-TolSO][(*R*)-Me-*p*-TolSO]Cl$_2$},[15] and the salt K{Pt[(*S*)-Me-*p*-TolSO]Cl$_3$}.[16] In the work presented herein we have determined the structure and absolute configuration of the *cis*- and *trans*-isomers of the mixed-ligand complex {Pt[(*S*)-Me-*p*-TolSO]PyCl$_2$} (Py, pyridine) and studied the chiroptical properties of the two isomers by CD spectroscopy. The synthetic methods were developed in our previous work.[11,16] A comparative study of the two isomers is of particular interest because of the difference in their catalytic properties in the hydrosilylation reaction, the *cis*-isomer being a more efficient catalyst.[1] For structurally similar neutral sulfoxide–quinoline complexes of the type [Pt(RR′SO)(quin)Cl$_2$] cytotoxic activity was reported[5] and different toxicities for the *cis*- and *trans*-isomers were found, the *trans*-isomer being the more toxic, implying mechanisms of action different from that of cisplatin. The strong and specific optical activity of the sulfoxide ligand may aid the elucidation of these mechanisms. For comparison, and to evaluate its use as a label, the uncomplexed chiral sulfoxide ligand was also studied by CD spectroscopy in various solvents.

* Corresponding author. Tel.: +7-812-2473740; fax: +7-812-2470341; e-mail: skvor@mail.cytspb.rssi.ru

0957-4166/02/$ - see front matter
PII: S0957-4166(02)00420-2

2. Results and discussion

2.1. Synthesis of complexes

In our previous work[11] we found that mixing equimolar quantities of aqueous solutions of (−)-*cis*-{Pt[(*S*)-Me-*p*-TolSO]$_2$Cl$_2$} and pyridine yields (−)-*cis*-{Pt[(*S*)-Me-*p*-TolSO]PyCl$_2$} **1A**.

From NMR studies,[18] it is known that in the reaction of *cis*-[Pt(DMSO)$_2$Cl$_2$] with pyridine in DMSO, the first step of the reaction is the formation of *trans*-[Pt(DMSO)PyCl$_2$]. This step is followed by a *trans* to *cis* isomerization of the complex. The preference for the *trans*-isomer in the first step of the reaction is usually explained on the basis of the *cis*-influence of the dimethylsulfoxide and pyridine ligands. Subsequent isomerization is then very effective in the presence of excess of DMSO (according to current opinion sulfoxide acts as a catalyst for isomerization).[19] So it may be assumed that the formation of **1A** also involves this isomerization process.

However, on monitoring the optical rotation of a mixture of equimolar *trans*-[Pt(Me-*p*-TolSO)PyCl$_2$] (**1B**) and Me-*p*-TolSO in CH_2Cl_2 at 20–40°C no changes in optical activity are detected for a number of hours. It is therefore improbable that *trans*-[Pt(Me-*p*-TolSO)PyCl$_2$] is an intermediate in the reaction of the bis-sulfoxide complex with pyridine. Sulfoxide-dependent isomerization is a very slow process, while the formation of **1A** from *cis*-[Pt(Me-*p*-TolSO)$_2$Cl$_2$] is complete in 5 min (according to polarimetric analysis). So in the present case the synthesis of **1A** does not include formation of **1B** with subsequent isomerization and the decay of a hypothetical cationic bis-sulfoxide pyridine intermediate *cis*-[Pt(Me-*p*-TolSO)$_2$PyCl]$^+$ yields the *cis*-isomer **1A** directly. The formation of a cationic intermediate is deduced from the combination of strong *cis*- and *trans*-influences of sulfoxide ligands in *cis*-[Pt(Me-*p*-TolSO)$_2$Cl$_2$].[14]

The only reliable method for the synthesis of (−)-*trans*-{Pt[(*S*)-Me-*p*-TolSO]PyCl$_2$} involves adding aqueous pyridine solution to an equimolar quantity of aqueous K{Pt[(*S*)-Me-*p*-TolSO]Cl$_3$}. This reaction is under kinetic control and yields the *trans*-isomer **1B**. The thermodynamically favored *cis*-isomer **1A** forms slowly if the reaction mixture is maintained at room temperature for a long period of time. ^{1}H NMR spectral analysis (comparing relative integrals of SCH_3 signals) shows that about 8% of **1B** is converted to **1A** at 20°C over 24 h, this process becomes more effective at higher temperature, where about 50% of the complex is converted to the *cis*-isomer during 2.5 h at 70°C.

2.2. X-Ray

X-Ray analysis of a series of Pt(II) complexes,[12–16] containing Me-*p*-TolSO and analogous methylphenylsulfoxide[20] prove that the chiral sulfoxide ligand is coordinated to platinum via the sulfur atom with retention of the relative position of substituents at the sulfur atom. In the present work we determined the structure of two more Me-*p*-TolSO complexes, *cis*- and *trans*-{Pt[(*S*)-Me-*p*-Tol-SO]PyCl$_2$} (**1A** and **1B**, respectively), by X-ray analysis. The bond lengths and angles for **1A** and **1B** are listed in Table 1. The molecular structure, absolute configuration, and atom numbering scheme is presented in Fig. 1.

The platinum atom in **1A** and **1B** is in an almost square-planar environment. The deviation of atoms from the coordination plane is less than 0.06 Å. The four angles of the coordination plane deviate slightly from 90°, the largest deviation (94.15(13)° between Pt–S and one of the Pt–Cl bonds) being observed in the *trans*-isomer. The chiral sulfoxide ligand is coordinated via sulfur and coordination causes notable shortening of S–O bond as compared to the free ligand. This shortening was also observed for other complexes studied. The lengths of the S–C bonds also change slightly. The coordinated sulfur atom has a distorted tetrahedral environment. The sum of the three bond angles at sulfur atom ($\angle OSC^{Me} + \angle OSC^{Me} + \angle C^{Me}SC^{Tol}$—the 'sulfoxide pyramid'), that equals 309.6(3)° in the free ligand[17] increases to 318.4(10)° in **1A** and up to 316.2(10)° in **1B** complex. Still, this is less than the 328.4° three bond angle sum in a regular tetrahedron. So the sulfoxide pyramid flattens upon coordination and the sulfur environment becomes more tetrahedral. In the *cis*-complex the oxygen atom of the sulfoxide ligand tends to enter the coordination plane (as indicated by Cl^1–Pt–S–O torsion) and points away from the *cis*-chloride ligand, following a trend, observed for *cis*-bis-sulfoxide platinum complexes,[15] whereas in the *trans*-complex, the oxygen atom is distinctly out of plane. The same orientation of sulfoxide with respect to the coordination plane was observed in the structurally analogous isomers, *cis*- and *trans*-[Pt(TMSO)(pm)Cl$_2$] (TMSO–teramethylenesulfoxide, pm-pyrimidine).[21]

The lengths of the Pt–ligand bonds in **1A** and **1B** are different. These bond lengths indirectly indicate that the mutual interaction of ligands differs between the *cis*- and *trans*-isomers. The Pt–S bond length has the intermediate value as compared to the shortest bond, observed in the salt K{Pt[(*S*)-Me-*p*-TolSO]Cl$_3$} and the longest bonds in the bis-sulfoxide complexes. The *trans*-influence of the sulfoxide ligand causes a small increase in the bond length *trans* to the Pt–S bond (Table 1). The Pt–N bond in the *cis*-isomer has a typical value for Pt–pyridine bonds *trans* to chloride (2.029(9) Å),[22,23] whilst in the *trans*-isomer this bond is longer. It is notable, that the major parameters of the coordination plane, including the angle distortions, almost coincide with the reported values for [Pt(TMSO)(pm)Cl$_2$] isomers,[22] though the sulfoxide geometries are certainly different. The studied complexes may also be compared with *cis*- and *trans*-[Pt(DMSO)PyCl$_2$] (DMSO–dimethylsulfoxide).[24,25] The increase in the bond length *trans* to sulfoxide in the Me-*p*-TolSO complexes is a little less than in the DMSO analogs. The Pt–S bond in the *cis*-isomer of the DMSO complex (2.209 Å)[25] is shorter than that in **1A**, while in the *trans*-isomers the Pt–S bond lengths are similar. The pyridine rings in

Table 1. Selected structural parameters for *cis*- and *trans*-{Pt[(*S*)-Me-*p*-TolSO]$PyCl_2$} complexes. Estimated standard deviations are given in parentheses

	cis-{Pt[(*S*)-Me-*p*-TolSO]$PyCl_2$}	*trans*-{Pt[(*S*)-Me-*p*-TolSO]$PyCl_2$}	(*R*)-Me-*p*-TolSO (data from Ref. 17)
Bonds (Å)			
Pt–N	2.032(10)	2.048(9)	
Pt–S	2.214(3)	2.225(3)	
Pt–Cl(1)	2.292(3)	2.299(3)	
Pt–Cl(2)	2.300(4)	2.290(3)	
S–O	1.469(10)	1.461(8)	1.493(10)
S–C(6)	1.809(13)	1.761(11)	1.797(7)
S–C(13)	1.769(14)	1.782(16)	1.796(13)
Angles (°)			
N–Pt–S	90.1(3)	177.3(2)	
S–Pt–Cl(1)	93.75(13)	88.92(12)	
S–Pt–Cl(2)	175.39(15)	94.14(13)	
N–Pt–Cl(2)	86.1(3)	87.4(3)	
N–Pt–Cl(1)	174.9(4)	89.6(3)	
Cl(2)–Pt–Cl(1)	90.17(15)	176.63(12)	
O–S–C(6)	108.6(6)	109.5(5)	106.5(3)
O–S–C(13)	108.3(7)	106.3(7)	105.5(3)
C(6)–S–C(13)	101.5(7)	100.4(7)	97.6(3)
O–S–Pt	115.5(4)	115.6(3)	
C(11)–C(6)–S	115.8(11)	119.2(10)	120.8(3)
C(7)–C(6)–S	121.6(11)	121.3(8)	118.8(3)
Dihedral angles (°)			
Cl(1)–Pt–S–O	−152.5(4)	53.3(4)	
O–S–C(6)–C(11)	8.6(13)	46.5(11)	5.0(15)

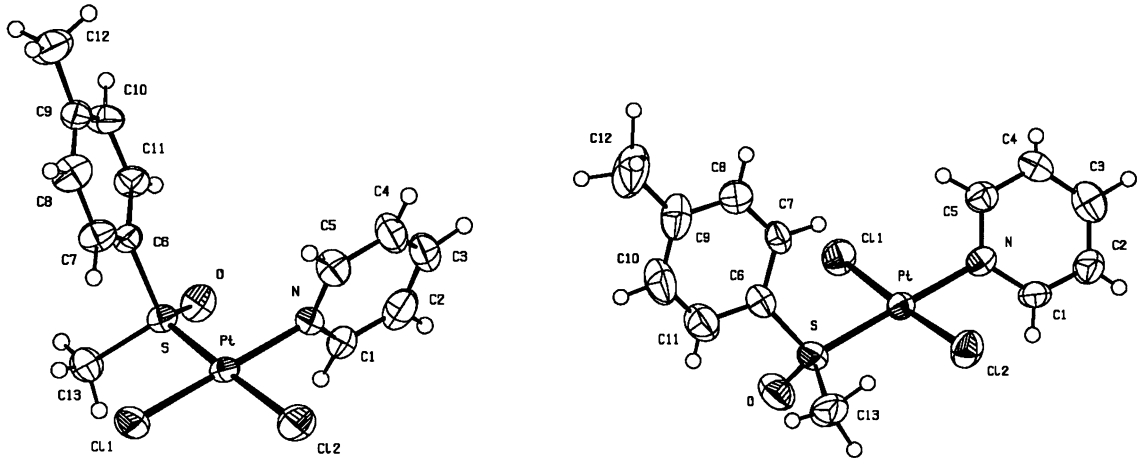

Figure 1. Crystal structure and absolute configuration of (–)-*cis*-{Pt[(*S*)-Me-*p*-TolSO]$PyCl_2$} (**1A**, left) and (–)-*trans*-{Pt[(*S*)-Me-*p*-TolSO]$PyCl_2$} (**1B**, right) (50% probability ellipsoids).

both complexes are flat and distorted to a small degree. The platinum atom in both complexes is located on the axis of symmetry of the pyridine ligand, which is indicative of unstrained coordination. The angle between the coordination plane and the plane of the pyridine ring is 77° in **1A** and 53° in **1B**. This observation follows the general trends for pyridine ligands, which try to achieve as much coplanarity as possible if no hindrance for the *ortho* hydrogens from other ligands, or packing forces are present.[22]

The structural characteristics of the *p*-tolyl group are fairly typical (taking standard deviations into account): in isomer **1A** the S–O bond is coplanar with the benzene ring, the same situation is known for the X-ray structure of the free ligand.[17] Such a configuration is favorable for sulfoxides with an *S*-aromatic substituent because of partial conjugation between the aromatic system and the electrons of the S–O bond.[26] However, the energy of this effect is fairly small −10 kCal/mol for the free ligand if no additional steric hindrance is

present (as evidenced by quantum calculations),[26] this situation is met in the complexes studied. So, conjugation of the S–O bond with the aromatic ring could be easily overridden by crystal packing requirements and thus it is not necessarily observed in X-ray structures of complexes with Me-*p*-TolSO. For instance in complex **1B** the S–O bond falls out of the tolyl plane and the dihedral angle OSC^6C^{11} equals 46.5(11)°. In the bis-sulfoxide complex (−)-*cis*-{Pt[(*S*)-Me-*p*-TolSO]$_2$Cl$_2$} only one ligand has a coplanar S–O bond, the other does not. The complementary chirality of ligands in the complex *cis*-{Pt[(*S*)-Me-*p*-TolSO][(*R*)-Me-*p*-TolSO]-Cl$_2$} allows the situation when both ligands have S–O bonds coplanar to the aromatic rings. Moreover, the rings themselves are almost parallel to each other.[15] The crystal lattice of the salt K[Pt[(*S*)-Me-*p*-TolSO]Cl$_3$] contains two structurally different types of anion. Conjugation of the S–O bond and the tolyl ring is observed for only one of them. The described conjugation is of interest, because it should significantly affect the spectral properties of Me-*p*-TolSO and the complexes.

Molecular modeling studies, based on X-ray values of bond lengths and angles, show that in complex **1B** both the pyridine and sulfoxide ligands can freely and independently rotate about the Pt–N and Pt–S bonds, respectively. In contrast, in complex **1A** only mutually correlated rotation of both ligands is possible.

The packing of complexes shows no peculiar intermolecular contacts or prominent stacking interactions, the *cis*-isomer is packed more densely. Alternating polar layers of platinum coordination planes and non-polar layers of aromatic rings are distinctly observed in crystal lattice of **1A**. These layers are perpendicular to the crystallographic axis *c*. No notable order was found in the crystal or **1B**.

2.3. NMR

The characteristic ^{1}H signals of the Me-*p*-TolSO and the pyridine ligands are shifted to low field upon coordination to platinum. As expected, the protons close to the donor site are more affected by coordination. The shifts are slightly larger in the *trans*-isomer for all signals, except those for the SCH_3 group (which are significantly more deshielded in the *cis*-isomer). The same trend for the sulfoxide protons is followed for mixed-ligand complexes with aliphatic sulfoxides.[21] The signals for the *ortho*-protons of pyridine and the SCH_3 signals are split by ^{195}Pt–^{1}H spin–spin coupling, resulting in a pseudotriplet pattern. The coupling constants $^3J_{195Pt-1H}$ are indicative of the complex geometry; in the *cis*-complexes they are distinctly larger than in the *trans*-complexes (*cis*-isomer: 24.5(4) Hz for SCH_3, 40.5(4) Hz for the *ortho*-pyridine protons; *trans*-isomer: 20.3(2) Hz, 34.0(3) Hz, respectively). This rule is followed not only in sulfoxide–pyridine complexes, but also in bis-sulfoxide and bis-pyridine complexes.[16,22] A peculiar property of proton signals, spin-coupled to ^{195}Pt, is the dependence of the shape on the applied magnetic field and temperature. This effect is due to the relaxation of ^{195}Pt nuclei, caused by strong chemical shift anisotropy of square-planar Pt(II) complexes. The relaxation rate for this effect is proportional to the square of the magnetic field. As the magnetic field is increased (or the temperature is decreased) this mechanism becomes dominant and causes broadening and collapse of signals from other nuclei (e.g. ^{1}H or ^{13}C), spin-coupled to platinum.[27,28] This effect should be especially important in Pt(II) complexes having bulky ligands, and it is almost negligible for Pt(IV) complexes with more symmetric electron density on platinum. For example, no valid ^{195}Pt splitting could be found in the 500 MHz proton spectra of **1A** and **1B**. The dependence of the relaxation rates on the magnetic field for isomers was studied by us earlier and the ^{195}Pt chemical shift anisotropy $|\sigma_{\parallel} - \sigma_{\perp}|$ was estimated to be about 2800 ppm for complex **1A**.[28]

2.4. UV and CD spectra

The stereogenic sulfur center is responsible for the strong circular dichroism (CD) of enantiomerically pure Me-*p*-TolSO and complexes that contain the Me-*p*-TolSO ligand. The stereogenic center of the sulfoxide appears to be configurationally stable and racemization does not occur under the influence of mild UV-irradiation or on heating to decomposition temperatures. Generally, sulfoxides display two electronic transitions of the S=O group that fall in the 200–260 nm region. These bands are broad and structureless, so the UV spectrum is not very informative. In chiral sulfoxides these transitions are optically active and show circular dichroism (CD) with opposite sign. This results in a characteristic two-band exciton-like pattern in CD spectrum (Fig. 2, dotted line). The sulfoxide moiety of Me-*p*-TolSO possesses significant inherent asymmetry, so it can be attributed to the first type of Moffit classification for optically active chromophores.[29] Both electronic and magnetic transition dipoles of such chromophores have non-zero values, which results in both high absorption and CD (Table 2). The conjugation of electrons of the S–O group and the aromatic (tolyl) ring is not negligible in Me-*p*-TolSO, so they cannot be considered as separate chromophores, and the whole ligand should be treated as a single chromophore. Yet the most intense pair of CD bands at 216 and 238 nm can be attributed to S–O group electronic transitions, since analogous bands are observed in the CD spectra of chiral sulfoxides bearing only alkyl substituents.[30] These two bands can be located in the UV-spectrum of the free ligand. They have opposite CD signs for chiral sulfoxides and their respective complexes. The absolute sign depends on the order of the substituents at the sulfur atoms. However, the reliable rules of CD sign determination, analogous to those for the carbonyl chromophore, have not been formulated yet. Since the sulfoxide CD spectrum is a result of partial compensation of two bands with opposite sign, their intensity should depend not only on rotational strength, but also on the relative band position, and thus should be solvent-dependent. When the solvent is gradually changed from ethanol to water, the low-energy band of Me-*p*-TolSO shows a strong blue shift and becomes more intense. In the CD spectrum these two trends act in opposite directions, thus, in contrast to the UV

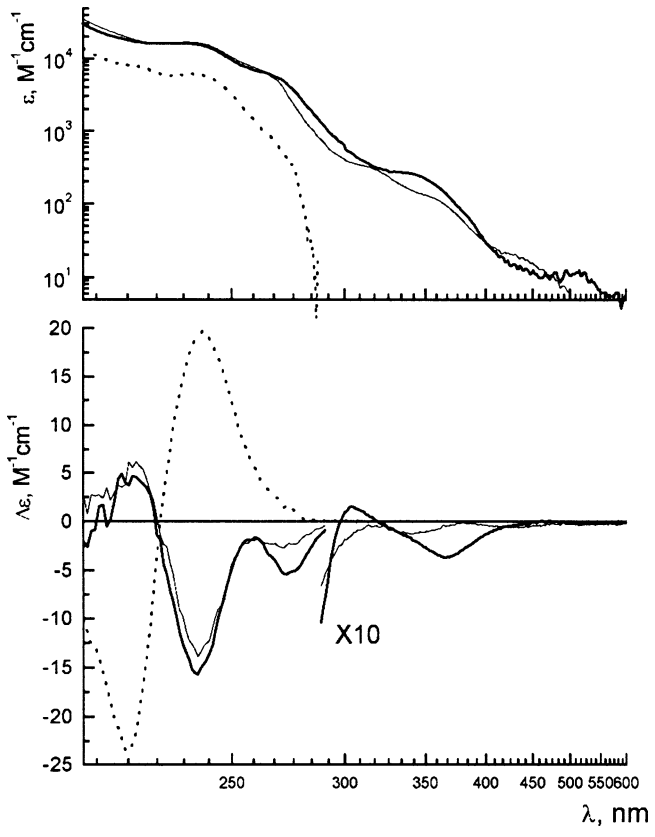

Figure 2. The UV and CD spectra of **1A** (thick line) and **1B** (thin line) and (+)-Me-*p*-TolSO (dotted line) at 20°C in 96% ethanol.

spectrum, the shape and intensity of the CD spectrum of Me-*p*-TolSO remain surprisingly conservative. The decrease in CD magnitude with increase in temperature from 10 to 60°C is less than 2%. Both isotropic and circular dichroic absorptions of Me-*p*-TolSO change linearly with concentration up to 1 mM (transparency limit). The transitions of the aromatic ring in aqueous and ethanolic solutions of (*R*)-Me-*p*-TolSO are observed in the CD and UV spectra as shoulder distortions at 270 nm and a small but sharp positive peak at 274.5 nm. In CH_2Cl_2 the shapes of the spectra are similar, but the low-energy band is very strongly red-shifted (the higher energy band could not be observed because of solvent absorption).

Inversion of the absolute configuration occurs at sulfur upon its coordination to platinum. As a consequence, the CD bands at 216 and 238 nm change sign (Fig. 2, Table 3). The overall environment at sulfur becomes more symmetrical (distorted tetrahedron in place of trigonal pyramidal), and the intensity of the CD bands decrease. The anisotropy factor $\Delta\varepsilon/\varepsilon$ decreases even more, as the UV absorption of complexes in 210–290 nm range is almost 2-fold higher than the absorption of the free ligand. The UV spectra of the complexes bear little information; the only easily detected feature is a broad peak at 235 nm, probably band(s) of coordinated sulfoxide. The CD bands are shifted upon coordination but the current data are too scarce to allow any relationships to be seen. The band at 275 nm becomes distinctly visible in the spectra of complexes and has a negative sign. Faint vibrational structure, typical of aromatic chromophore transitions is observed in ethanol solutions of complexes **1A** and **1B**. The position and intensity of this band depends on the geometry of the complex in a more profound way than the 238 nm band. The 275 nm band in **1A** is clearly shifted to longer wavelength as compared to **1B**. We suggest that this band arises from the induced optical activity of the rotation-hindered tolyl ring, though pyridine ring transitions cannot be ruled out. In the *trans*-complex pyridine and sulfoxide ligands can easily rotate about ligand–platinum bonds. The induced asymmetry is partly averaged out, so the intensity of the 275 nm CD band decreases. Our suggestion is consistent with the observed CD spectra of analogous neutral complexes (−)-*cis*-[Pt(Me-*p*-TolSO)(Bu_3P)Cl_2] and (−)-*cis*-[Pt(Me-*p*-TolSO)(NH_2Me)Cl_2] that bear no aromatic groups except the tolyl ring (Table 3). The large Bu_3P ligand in the *cis* position should hinder the movement of the sulfoxide ligand, this results in higher CD at 275 nm. In contrast the small NH_2Me ligand permits free rotation of the Me-*p*-TolSO ligand, the induced optical activity averages out, and the CD decreases.

The platinum complexes with chiral Me-*p*-TolSO also show several weak and broad CD bands at wavelengths above 300 nm that stretch to the visible region, like those shown in Fig. 2 for **1A** and **1B**. For complex **1B** the CD can be detected above 500 nm. Unfortunately, the corresponding UV bands are almost completely masked by shoulders of higher energy UV-absorption bands. The low-energy CD bands originate from the induced optical activity of *d*–*d* transitions on platinum.[31] The chiral ligand can rotate with respect to the coordination plane, and the sign of the induced optical activity should be different for various conformers of the complex. As the solution is a dynamic mixture of conformers, the observed spectrum should be a result of the CD of various conformers and the distorted band shapes are indicative of this. Thus, the number of peaks and their positions doesn't necessarily correlate with the number and energy of *d*–*d* transitions. The absorption of the *trans*-complex **1B** stretches further into the visible region, as compared to **1A**, resulting in a deeper color of **1B** (and complies with general rules for sulfoxide–pyridine platinum complexes). The *d*–*d* region is very sensitive to the absolute configuration at the platinum atom, but the low intensity and large bandwidths make this region unsuitable for dynamic studies.

We would like to note, that the CD spectra of bis-sulfoxide complexes differ greatly from the pattern described for complexes with one sulfoxide ligand (Table 3). The most likely reason for this difference is mutual hindrance and dipole–dipole interaction of the two sulfoxides, which results in exciton doubling of the CD bands (as is well known for polynucleotides).[32] Therefore, the CD spectrum depends not only on the inherent optical activity of chromophores but also on their preferred mutual orientation. An analogous mech-

Table 2. UV and CD spectral data for (+)-(*R*)-Me-*p*-TolSO in water–ethanol mixtures and in CH_2Cl_2 (20°C, sulfoxide concentration used: 2×10^{-5} to 2×10^{-4} M)[a]

Solvent	UV absorption λ, nm [$\varepsilon\times10^{-3}$, M^{-1} cm^{-1}]	Circular dichroism λ, nm [$\Delta\varepsilon$, M^{-1} cm^{-1}]
Pure water, or ethanol less than 10% vol.		200 [−22.0(12)]
	222 [8.0(2)]	**216.0 [−20.2(5)]**
		225.0 [0.0(3)]
	230 [8.1(2)]	**237.5 [+19.0(5)]**
	274.4 [0.43(3)]	274.0 [+0.8(1)]
20% vol. ethanol	**221.5 [8.5(2)]**	**216.0 [−21.5(5)]**
		225.2 [0.0(4)]
	231 [8.4(2)]	**238.0 [+20.2(4)]**
	274.7 [0.42(3)]	274.0 [+0.9(1)]
40% vol. ethanol[b]	**219.5 [8.4(2)]**	**216.2 [−23.0(7)]**
		225.3 [0.0(5)]
	232.6 [8.0(2)]	**238.8 [+21.1(6)]**
	274.7 [0.40(3)]	274.0 [+1.0(1)]
96% vol. ethanol	**217 [8.0(3)]** shoulder	**216.5 [−23.9(5)]**
		226 [0.0(5)]
	237 [6.1(3)]	**240.2 [+19.5(5)]**
	275 [0.32(2)] shoulder	274.5 [+1.3(2)]
CH_2Cl_2	222[c] [14.5(2)]	222[c] [−45(2)]
	234 [5.4(1)] through	230.7 [0.0(5)]
	244.5 [6.5(1)]	**246.0 [+26(1)]**

[a] Estimated standard deviations are given in parentheses
[b] The CD, but not UV spectra are almost invariable with ethanol concentration ranging from 40 to 85% vol.
[c] This value does not correspond to any peak, it is the last reliable point below transparency edge of the sample

anism may be responsible for the complex spectrum of (−)-*cis*-{Pt[(*S*)-Me-*p*-TolSO](Ph$_3$PS)Cl$_2$} which bears a bulky triphenylphosphinesulfide ligand with aromatic chromophores.

The optical rotation, used by us to monitor a number of reactions of chiral sulfoxide complexes[9–11] is mainly determined by the low-energy sulfoxide CD band, which is positive for the free sulfoxide and causes positive $[\alpha]_D$ (+142, in CH_2Cl_2), but is negative for the *S*-coordinated sulfoxide, resulting in negative $[\alpha]_D$ values. The lower energy transitions affect mostly the magnitude but not the sign of the optical rotation (Table 3).

In a non-polar solvent such as CH_2Cl_2 the spectral bands of **1A** and **1B** exhibit red shifts, but for the 238 nm band it is more moderate than in the free ligand, probably because the coordinated sulfur atom is no longer exposed to solvent. In freshly prepared aqueous solutions the spectra of **1A** and **1B** change and the bands are blue-shifted. Other general trends are the decrease in intensity of 238 nm sulfoxide band (opposite to the behavior of the free sulfoxide) and the complete disappearance of vibrational structure. While 4×10^{-4} M solutions in ethanol are stable for several months if stored in the dark at 20°C, as evidenced by their UV and CD spectra, the spectra of aqueous solutions change with time, indicating hydrolysis. The *trans*-isomer converts over several hours at 35°C in a two-step reaction to other species, yet the sulfoxide in these species is still coordinated, as the CD at 238 nm is negative. The species formed is stable for days and no sulfoxide is released. In contrast, the *cis*-isomer releases the sulfoxide ligand very slowly. There is much indirect evidence, e.g. the influence of Cl^- concentration on the CD spectra, that even in fresh ethanol solutions the chloride ligand of **1A** *trans* to sulfoxide rapidly exchanges with residual water. The nature of the hydrolysis products and hydrolysis rates are currently under study. It should be noted that over time 2×10^{-5} M solutions in ethanol show the same but slower hydrolysis effects as aqueous solutions, as judged by CD-difference spectra. This fact could be explained by the higher water to complex ratio in such solutions. As some sulfoxide complexes are potential photocatalysts,[9] several attempts were made to study the influence of visible light and UV-beam of the dichrograph on the stability of the solutions to estimate photolysis and/or photoisomerization. Unfortunately the observed changes are below the experimental error. It is known, that some mixed-ligand sulfoxide–pyridine complexes isomerize from *trans*- to *cis*-geometry in organic solvents.[21] No detectable isomerization of {Pt[(*S*)-Me-*p*-TolSO)]PyCl$_2$} was observed either by NMR studies in $CDCl_3$, or UV and CD spectroscopy in ethanol, and we may conclude that this complex is stable to isomerization. The isomerization may still be induced by stronger UV-irradiation (*cis* to *trans*), prolonged heating in toluene (*trans* to *cis*) or by adding nucleophiles (e.g. DMSO) in non-polar solvents.[11]

The addition of NaCN causes the rapid substitution of all ligands and formation of $[Pt(CN)_4]^{2-}$. This reaction could be used as a simple way to measure the actual content of chiral sulfoxide in the system by CD spectroscopy, as the sulfoxide contains the only stable stereogenic center and all other components have zero optical activity. In our experiments the spectra of mixtures formed in the reaction with NaCN matched the spectra of the pure sulfoxide perfectly. The sulfoxide concentrations calculated from CD spectra were in good agreement with the expected values, within experimental error.

3. Conclusion

We have obtained the *cis*- and *trans*-isomers of optically active mixed-ligand complexes (−)-[Pt(Me-*p*-TolSO)PyCl$_2$] and characterized them by crystallographic methods, ^{1}H NMR, UV and CD spectroscopy. The studied isomers showed no spontaneous isomerization (reported for some other mixed-ligand sulfoxide complexes), as judged by NMR and CD spectroscopy. X-Ray analysis confirms the coordination via sulfur with the retention of the relative order of substituents at sulfur and inversion of absolute configuration. Platinum–ligand bond lengths indicate the

Table 3. Major CD and UV spectral properties of Pt(II) complexes with chiral Me-*p*-Tol-SO ligand, 20°C in various solvents

Compound	Solvent	CD spectrum λ_{peak}, nm [$\Delta\varepsilon$, M^{-1} cm^{-1}]	UV spectrum λ, nm [$\varepsilon\times10^{-3}$, M^{-1} cm^{-1}]	Optical rotation[a] $[\alpha]_D^{20}$
(−)-*cis*-{Pt[(*S*)-Me-*p*-TolSO]$PyCl_2$}	Ethanol	218 [+4.6], **238.5 [−15.6]**, **272.5 [−5.0]**, 304 [+0.16], 366 [−0.37].	234.5 [16.4], 262 [6.4] shoulder, 332 [0.28].	
(−)-*trans*-{Pt[(*S*)-Me-*p*-TolSO]$PyCl_2$}	Ethanol	219 [+6.0], **240.0 [−13.7]**, **271.0 [–2.8]**, 342 [−0.13], 435 [−0.05].	235 [16.8], 260 [7.3] shoulder, 347 [0.13] shoulder.	
(−)-*cis*-{Pt[(*S*)-Me-*p*-TolSO]$(Bu_3P)Cl_2$}	Ethanol	220 [+18.8], **237.7 [−11.8]**, **272 [−4.9]**, 332 [−0.7].		−37 (in CH_2Cl_2)
(−)-*cis*-{Pt[(*S*)-Me-*p*-TolSO]$(NH_2Me)Cl_2$}	Ethanol	215 [+2.9], **237.5 [−11.5]**, **273 [−1.6]**.		
(−)-*cis*-{Pt[(*S*)-Me-*p*-TolSO]$PyCl_2$}	CH_2Cl_2	220 [+8], **241 [−22.3]**, **277 [−6.8]**, 305 [+0.16], 370 [−0.50].	238 [19.6], 264 [8.0] shoulder, 338 [0.36] shoulder.	−117
(−)-*trans*-{Pt[(*S*)-Me-*p*-TolSO]$PyCl_2$}	CH_2Cl_2	220 [+4], **241 [−17.3]**, **272 [−3.8]**, 345 [−0.2], 440 [−0.09].	239 [18.9], 261 [9.1] shoulder, 347 [0.15] shoulder.	−22
(−)-*cis*-[Pt(*S*)-Me-*p*-$TolSO]_2Cl_2$}	CH_2Cl_2	252.5 [−28], 275 [+2.0], 290 [−4.3], 320 [+2.3], 360 [−0.4].		−220
(−)-*cis*-{Pt[(*S*)-Me-*p*-TolSO]$(Ph_3PS)Cl_2$}	CH_2Cl_2	225 [+2], 245 [−21], 270 [+4.1], 297 [−3.7].		−121[b]

[a] Values from Ref. 16.
[b] Our data

expected high *trans*-influence of sulfoxide. Based on the X-ray data we may conclude that in the *cis*-isomer, the sulfoxide and pyridine ligands are mutually hindered, while in the *trans*-isomer they may rotate freely, this may contribute to the different optical activity of the isomers.

The stereogenic center remains stable on coordination and is well-detectable by CD spectroscopy. The two optically active electronic transitions of the free sulfoxide, most probably affecting the electrons of the S–O group, change the sign of the optical activity upon coordination. The sign of the optical rotation changes correspondingly. Substitution of sulfoxide with other nucleophiles causes reappearance of the initial sign of optical activity and may serve as a good instrument for ligand substitution studies by CD spectroscopy. This method has an advantage over UV spectroscopy as the chiral sulfoxide ligand is the only significant contributor to circular dichroism in the system. The magnitude of CD is high enough to detect it at micromolar concentrations. Even the substitution reactions with amino acids and DNA may be studied, as Me-*p*-TolSO optical activity is comparable to that of DNA, and the optical activity of free and coordinated amino acids at wavelengths above 220 nm is negligible. The near-UV bands of complexes are sensitive to the nature of the other ligands, and their change may witness substitution of ligands. The CD spectrum of free chiral sulfoxide is quite conservative and change moderately when changing solvent from ethanol to water. Together with the small dependence of CD on temperature, this fact makes Me-*p*-TolSO a good chiral label for studies of substitution reactions at concentrations relevant to catalytic and biological systems.

4. Experimental

4.1. Materials

The chiral sulfoxide (+)-*R*-Me-*p*-TolSO was synthesized by the method described in literature.[33] The enantiomeric purity of this ligand exceeded 96%. (−)-*cis*-{Pt[(*S*)-Me-*p*-TolSO]$PyCl_2$} **1A** and (−)-*trans*-{Pt[(*S*)-Me-*p*-TolSO]$PyCl_2$} **1B** (molecular mass 499.31) were synthesized from K_2PtCl_4, pyridine and (*R*)-(+)-Me-*p*-TolSO via [Pt(Me-*p*-$TolSO)_2Cl_2$] and K[Pt(Me-*p*-$TolSO)Cl_3$], respectively, using the methods, described earlier[11] and recrystallized from acetone. Melting points: *cis*-isomer 163°C, *trans*-isomer 151.5°C. (−)-*cis*-{Pt[(*S*)-Me-*p*-TolSO]$(Bu_3P)Cl_2$} and (−)-*cis*-{Pt[(*S*)-Me-*p*-TolSO] $(NH_2Me)Cl_2$} were synthesized by published methods.[16] Methylene chloride was obtained from 'Merck' and used without purification. Distilled ethanol (azeotropic) and double-distilled deionized water were used for UV/CD measurements, pH was not controlled, initially it was 5.0.

4.2. X-Ray

The crystals of **1A** and **1B** were grown from acetone solutions. The X-ray diffraction data were obtained with Enraf–Nonius CAD4 diffractometer with Nb β-filtered MoK_α source (0.71073 Å). The $\theta/2\theta$ scan with $2\theta_{max}=50°$ was used. The intensities of three selected

reflections, monitored each 60 min showed a decay less than 1.6% during the experiment. The temperature of the crystals was (293±2) K.

The colorless crystal of **1A**, 0.42×0.22×0.14 mm, was used for analysis. **1A** crystallizes in $P2_12_12_1$ orthorhombic space group. The unit cell parameters are: $a=5.877(1)$, $b=14.003(3)$, $c=18.651(4)$ Å, $V=1534.9(5)$ Å^3, $Z=4$, $\rho_{calcd}=2.161$ g cm^{-3}, $F(000)=944$. The data were collected in *hkl* range 0–6, 0–16, 0–22; 1034 reflections with $I>3\sigma(I)$ were measured. X-Ray absorption, $\mu=96.16$ cm^{-1}, was accounted for. Non-hydrogen atoms were refined anisotropically by full-matrix least-squares method on *F*. The hydrogen atoms were added at arbitrary positions and refined isotropically. Final $R=0.040$, $R_w=0.094$ for all observed reflections.

The orange crystal of **1B**, 0.46×0.22×0.05 mm, was studied. **1B** crystallizes in $P2_12_12_1$ orthorhombic space group. The unit cell parameters are: $a=7.287(1)$, $b=8.781(1)$, $c=25.032(5)$ Å, $V=1601.7(5)$ Å^3, $Z=4$, $\rho_{calcd}=2.071$ g cm^{-3}, $F(000)=944$. The data were collected in *hkl* range 0–6, 0–10, 0–28; 1091 reflections with $I>3\sigma(I)$ were measured. X-Ray absorption, $\mu=92.15$ cm^{-1}, was accounted for. Non-hydrogen atoms were refined anisotropically by full-matrix least-squares method on *F*. The position of hydrogen atoms were determined from difference syntheses and refined isotropically. Final $R=0.014$, $R_w=0.049$ for all observed reflections.

Crystallographic data (excluding structure factors) for the structures in this paper have been deposited with the Cambridge Crystallographic Data Centre as supplementary publication numbers CCDC 185014 and 185015. Copies of the data can be obtained, free of charge, on application to CCDC, 12 Union Road, Cambridge, CB2 1EZ, UK (fax: +44(0)-1223-336033; e-mail: deposit@ccdc.cam.ac.uk or www.ccdc.cam.ac.uk).

4.3. NMR

The ^{1}H NMR spectra of **1A** and **1B** were recorded from $CDCl_3$ saturated solutions at 200.13 MHz on a Bruker AC-200 spectrometer in standard 5 mm NMR tubes. No internal standard was used, the ^{1}H chemical shifts in ppm from TMS were calculated from deuterium lock frequency. Other parameters: 40° pulses, 8K data points; resolution, 0.61 Hz; 50–100 scans. ^{1}H NMR spectra δ, ppm: **1A**: 2.44 s (3H, CH_3); 3.58 t (3H, SCH_3), $^3J_{H-Pt}$ 24.6 Hz; 7.94 d (2H, H$^{\alpha}$[Tol]), 7.38 d (2H, H$^{\beta}$[Tol]), ^3J 8.1 Hz; 8.62 m (2H, H$^{\alpha}$[Py]), $^3J_{H-Pt}$ 40.5 Hz; 7.30 m (2H, H$^{\beta}$[Py]); 7.80 m (1H, H$^{\gamma}$[Py]); $^3J_{\alpha-\beta}$ 5.7 Hz, $^3J_{\beta-\gamma}$ 8.0 Hz, $^4J_{\alpha-\gamma}$ 1.3 Hz; **1B**-2.47 s (3H, CH_3); 3.46 t (3H, SCH_3), $^3J_{H-Pt}$ 20.3 Hz; 7.96 d (2H, H$^{\alpha}$[Tol]), 7.40 d (2H, H$^{\beta}$[Tol]), ^3J 8.2 Hz; 8.79 m (2H, H$^{\alpha}$[Py]), $^3J_{H-Pt}$ 34 Hz; 7.42 m (2H, H$^{\beta}$[Py]); 7.86 m (1H, H$^{\gamma}$[Py]); $^3J_{\alpha-\beta}$ 5.7 Hz, $^3J_{\beta-\gamma}$ 8.1 Hz, $^4J_{\alpha-\gamma}$ 1.3 Hz.

4.4. UV–vis and CD spectra

The UV–vis absorption spectra were obtained on scanning spectrophotometer Specord-M40 (Karl Zeiss, Germany). CD spectra were recorded with dichrograph Mark-V (Jobin-Yvon, France) and with spectropolarimeter-dichrograph Cary-60M (Varian, USA). (+)-10-D-Camphorsulfonic acid was used as calibration standard for CD measurements. The fused silica quartz cells with optical pathlength 1, 0.5 and 0.1 cm were used. The external thermostat allowed to control the temperature in the range 10–60°C. Absorbance of solvent and optical activity of cell walls were accounted for. Crystals of complexes **1A** and **1B** (sample mass about 2.5±0.05 mg) were dissolved in acetone in concentration 10^{-3} M and divided into small equal volumes. Then acetone was evaporated in dry nitrogen flow and the formed powder was redissolved in ethanol up to concentration 4×10^{-4} M. This solution was further diluted with ethanol or water to yield the samples, suitable for CD and UV measurements. This procedure was used to shorten the time of sample preparation, and to reduce the possibility for isomerization and hydrolysis. The large crystals of complexes dissolve only very slowly in ethanol, but the fine powder is dissolved rapidly. The spectra of solutions (except of CH_2Cl_2) were recorded from at least three independently prepared samples, their shapes were found to be perfectly identical, and the presented magnitudes of ε and $\Delta\varepsilon$ are median values. Solutions of Me-*p*-TolSO in water–ethanol mixtures were prepared with 10% vol. increment in ethanol content.

4.5. The substitution of chiral sulfoxide

The aqueous and ethanol solutions of complexes **1A** and **1B** used for CD and UV spectroscopy with typical concentrations ranging from 4×10^{-4}M to 1×10^{-5} M were mixed directly in the 1 cm CD-cell (2 ml) with small volumes of aqueous 0.01 M NaCN resulting in about 10-fold excess of CN^- over platinum. Larger excess was avoided to keep the solution transparent for far-UV. Several cases with lowest concentrations were monitored by CD spectroscopy, and reactions were found to be complete in 1–5 min at 20°C.

Acknowledgements

This work was supported by the Russian Foundation for Basic Research, grants nos. 00-03-32578a, 01-03-32598a (financial support) and 99-07-90133 (access to CCDC database).

References

1. De Vekki, D. A.; Ol'sheev, V. A.; Spevak, V. N.; Skvortsov, N. K. *Russ. J. Gen. Chem.* **2001**, *71*, 1912–1923.
2. Trofimov, A. E.; Skvortsov, A. N.; Pashnova, L. V.; Skvortsov, N. K. *Russ. J. Gen. Chem.* **1998**, *68*, 572–577.
3. Lasitsa, N. A.; Skvortsov, N. K.; Lobadyuk, V. I.; Spevak, V. N.; Yesina, G. A.; Abramova, I. P.; Lazarev, S. Ya. *Russ. J. Gen. Chem.* **1992**, *62*, 1533–1536.

4. Trofimov, A. E; Spevak, V. N.; Lobadyuk, V. I.; Skvortsov, N. K.; Reikhsfel'd, V. O. *Russ. J. Gen. Chem.* **1989**, *59*, 1837–1840.
5. Van Beusichem, M.; Farrell, N. *Inorg. Chem.* **1992**, *31*, 634–639.
6. Farrell, N.; Kinley, D. M.; Schmidt, W.; Hacker, M. P. *Inorg. Chem.* **1990**, *29*, 397–403.
7. Sacht, C.; Datt, M. S.; Otto, S.; Roodt, A. *J. Chem. Soc., Dalton Trans. 1* **2000**, 727–733.
8. Lobadyuk, V. I.; Spevak, V. N.; Skvortsov, N. K. *Russ. J. Gen. Chem.* **1996**, *66*, 849.
9. Spevak, V. N.; de Vekki, D. A.; Skvortsov, N. K. *Russ. J. Appl. Chem.* **2001**, *6*, 921–924.
10. De Vekki, D. A.; Spevak, V. N.; Skvortsov, N. K. *Russ. J. Gen. Chem.* **2000**, *70*, 1240–1242.
11. De Vekki, D. A.; Spevak, V. N.; Skvortsov, N. K. *Russ. J. Coord. Chem.* **2001**, *27*, 579–584.
12. Ball, R. G.; Payne, N. C. *Inorg. Chem.* **1976**, *15*, 2494–2498.
13. Ball, R. G.; Payne, N. C. *Inorg. Chem.* **1977**, *16*, 1871–1875.
14. Spevak, V. N.; Skvortsov, N. K.; Belsky, V. K.; Konovalov, V. E.; Lobadyuk, V. I. *Russ. J. Gen. Chem.* **1992**, *62*, 2183–2187.
15. Fanizzi, F. P.; Natile, G.; Lanfranchi, M.; Tiripicchio, A. *Inorg. Chim. Acta* **1997**, *264*, 11–18.
16. Spevak, V. N.; Lobadyuk, V. I.; Skvortsov, A. N.; Konovalov, V. E.; Bel'sky, V. K.; Skvortsov, N. K. *Russ. J. Gen. Chem.* **1999**, *69*, 715–720.
17. De la Camp, U.; Hope, H. *Acta Crystallogr., Sect. B.* **1970**, *26*, 852.
18. Kong, P.-C.; Iyamuremye, D.; Rochon, F. D. *Can. J. Chem.* **1976**, *54*, 3224–3226.
19. Price, J. H.; Birk, J. P.; Wayland, B. B. *Inorg. Chem.* **1978**, *17*, 2245–2250.
20. Antolini, L.; Folli, U.; Iarossi, D.; Schenetti, L.; Taddei, F. *J. Chem. Soc., Perkin Trans. 2* **1991**, 955.
21. Nedelec, N.; Rochon, D. F. *Inorg. Chim. Acta* **2001**, *319*, 95–108.
22. Tessier, C.; Rochon, F. D. *Inorg. Chim. Acta* **2001**, *322*, 37–46.
23. Tessier, C.; Rochon, F. D. *Inorg. Chim. Acta* **1999**, *295*, 25–38.
24. Caruso, F.; Spagna, R.; Zambonelli, L. *Acta Crystallogr., Sect. B* **1980**, *36*, 713.
25. Belsky, V. K.; Konovalov, V. E.; Kukushkin, V. Yu. *Acta Crystallogr., Sect. C (Cr. Str. Comm.)* **1991**, *47*, 292.
26. Benassi, R.; Mucci, A.; Schenetti, L.; Taddei, F. *J. Mol. Struct.* **1989**, *184*, 261–268.
27. Ismail, I. M.; Kerrison, S. J.; Sadler, P. J. *Polyhedron* **1982**, *1*, 57–59.
28. Skvortsov, A. N. *Russ. J. Gen. Chem.* **2000**, *70*, 1023–1027.
29. Moffit, W.; Moskowitz, A. *J. Chem. Phys.* **1959**, *30*, 648–660.
30. Drabowicz, J.; Dudzinski, B.; Mikolajczyk, M. *J. Chem. Soc., Chem. Commun.* **1992**, 1500–1502.
31. Scott, A. I.; Wrixton, A. D. *Tetrahedron* **1971**, *27*, 2339–2369 and references cited therein.
32. Tinoco, I.; Bustamante, C., Jr.; Maestre, M. F. *Annu. Rev. Biophys. Bioeng.* **1980**, *9*, 107–141.
33. Drabowics, J.; Bujnicki, B.; Mickolajczyk, M. *J. Org. Chem.* **1982**, *47*, 3325.